Available online at www.sciencedirect.com
ScienceDirect
C. R. Physique 8 (2007) 449–455
COMPTES RENDUS PHYSIQUE
http://france.elsevier.com/direct/COMREN/

Physics/Mathematical physics, theoretical physics

Herzfeld instability versus Mott transition in metal–ammonia solutions

Gennady N. Chuev [a,b], Pascal Quémerais [c,*]

[a] *Institute of Theoretical and Experimental Biophysics, Russian Academy of Sciences, Pushchino, Moscow Region, 142290, Russia*
[b] *School of Physics, The University of Edinburgh, Mayfield Road, Edinburgh EH9 3JZ, United Kingdom*
[c] *Institut Néel, CNRS, BP 166, 38042 Grenoble cedex 9, France*

Received 15 January 2007; accepted after revision 9 May 2007

Available online 20 June 2007

Presented by Jacques Vilain

Abstract

Although most metal–insulator transitions in doped insulators are generally viewed as Mott transitions, some systems seem to deviate from this scenario. Alkali metal–ammonia solutions are a brilliant example of this. They reveal a phase separation in the range of metal concentrations where a metal–insulator transition occurs. Using a mean spherical approximation for quantum polarizable fluids, we argue that the origin of the metal–insulator transition in such a system is likely to be similar to that proposed by Herzfeld a long time ago, namely, due to fluctuations of solvated electrons. We also show how the phase separation may appear: the Herzfeld instability of the insulator occurs at a concentration for which the metallic phase is also unstable. As a consequence, the Mott transition cannot occur at low temperature. The proposed scenario may provide a new insight into the metal–insulator transition in condensed-matter physics. ***To cite this article: G.N. Chuev, P. Quémerais, C. R. Physique 8 (2007).***

Résumé

Instabilité de Herzfeld versus transition de Mott dans les solutions de métaux dans l'ammoniac. Bien que la plupart des transitions isolant–métal dans les semiconducteurs dopés soient interprétées comme des transitions de Mott, certains systèmes semblent échapper à ce scénario. Les solutions de métaux alcalins dans l'ammoniac en sont un brillant exemple. Elles présentent une séparation de phase dans la gamme de concentration pour laquelle la transition isolant–métal se produit. En utilisant des approximations adéquates pour les fluides quantiques polarisables, nous montrons que l'origine de la transition isolant–métal dans ce système est probablement similaire à celle proposée il y a longtemps par Herzfeld, c'est-à-dire, due aux fluctuations des électrons solvatés. Nous montrons également pourquoi la séparation de phase peut apparaître : l'instabilité de Herzfeld de l'isolant se produit à une concentration pour laquelle la phase métallique est aussi instable. En conséquence, la transition de Mott ne peut pas se produire à basse température. Le scénario proposé ouvre de nouvelles perspectives pour la transition isolant–métal en physique de la matière condensée. ***Pour citer cet article : G.N. Chuev, P. Quémerais, C. R. Physique 8 (2007).***

Keywords: Solvated electrons; Mott transition; Phase separation

Mots-clés : Electrons solvatés ; Transition de Mott ; Séparation de phase

* Corresponding author.
E-mail addresses: genchuev@rambler.ru (G.N. Chuev), pascal.quemerais@grenoble.cnrs.fr (P. Quémerais).

1631-0705/$ – see front matter
doi:10.1016/j.crhy.2007.05.016

1. Introduction

In his theory of metalization, Herzfeld [1], following previous studies of Goldhammer [2], has considered dipolar fluctuations of neutral atoms as the origin of a metal–insulator transition (MIT). He emphasized that the restoring force of an electron bound to an atom collapses and the substance becomes metallic at increased densities due to local field effects. Despite some successful examples of applications [3–6], serious doubts arose because most of the experiments gave evidence in favor of the Mott scenario [7]. The two theories are based on very different effects, since Mott considered the MIT from the metallic side of the transition, whereas Herzfeld investigated the same phenomenon from the insulating one. Recent studies on a Wigner crystal formed by large polarons have, however, opened new perspectives for the Herzfeld idea [8,9]. Motivated by these studies, we argue that a modified Herzfeld approach may provide a key to understand the MIT in certain real systems. In particular, we focus in this paper on the metal–ammonia solutions (MAS). Although it is a century-old problem [10], the phase diagram of MAS (see Fig. 1) has remained mysterious up to now. Many studies have been performed and a large volume of experimental data have been accumulated about this fascinating system (for review, see [12,13]). Once an alkali metal is dissolved in liquid ammonia, it immediately dissociates to give two separated entities with unlike charges: the solvated ions and the excess electrons. At low metal concentration, the solution remains non-metallic (electrolytic) and has an intense blue colour independently on the type of alkali metal. Jortner [14] argued that due to short-range interactions with ammonia molecules, an excess electron forms a cavity free of solvent in which it localizes with the help of the polarization carried by the surrounding ammonia molecules. This process results in a trap formation similar to that for the polarons in solids. The radius of the cavity has been estimated to be $r_c \approx 3.2$ Å [14]. Modern theories based on path integral simulations [15], or on the density functional approach [16,17] provide an evaluation of the microscopic structure around solvated electrons but they all yield the same physical picture as that described above. At large enough metal concentration, the MAS becomes a liquid metal with a typical bronze coloration. However, at concentrations varying from 1 to 10 mole percent of metal (MPM), a separation between the low density blue phase and the higher density bronze one takes place, resulting in a miscibility gap below a critical temperature (Fig. 1). Importantly, the phase separation occurs for Li, Na, or K, but was not observed in the case of Cs. However, for all type of alkali metal, many experimental data reveal the presence of a MIT in the same range of densities [12], as reported in Fig. 1 for the case of Na. Earlier models considering the Mott mechanism [18] or involving an association of localized electrons in clusters [19] were not able to explain the whole phase diagram observed in MAS satisfactorily. What is the reason? From an electrostatic point of view, solvated electrons behave more or less like some solvated anions,

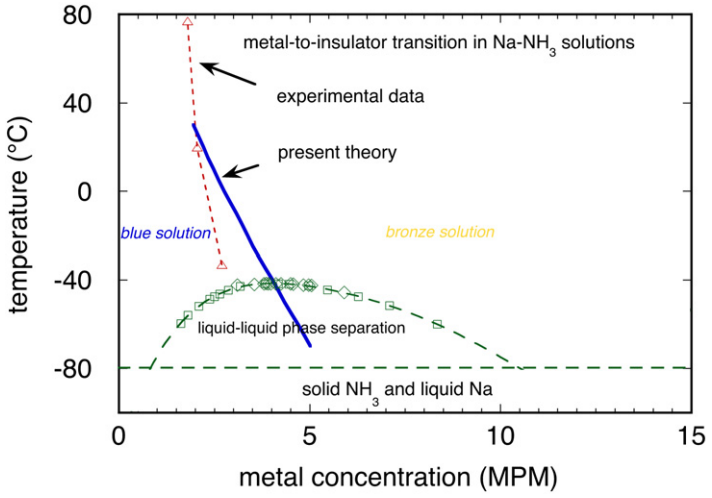

Fig. 1. Phase diagram of Na–NH_3. The experimental data on the locus of the phase separation are indicated by the square [10] and diamond symbols [11], respectively. The triangles show the change in sign of the derivative of the conductivity coefficient $d\sigma/dT$, which is used to estimate the locus of the MIT [12]. The solid curve corresponds to our calculations of the locus of the polarization catastrophe. All dotted curves are guides for the eyes, except the dashed horizontal line at $T = -80\,^{\circ}\mathrm{C}$ indicating the solidification temperature of ammonia. [1(MPM) $\approx 2 \times 10^{20}$ cm^{-3}.]

the counterpart of the solvated metal cations. The Debye screening length $\ell_D = (8\pi\beta ne^2/\epsilon_s)^{-1/2}$ is found to be about 1 Å at 4 MPM and $T = -40\,^{\circ}\mathrm{C}$. Here n is the density of metal atoms, β is the inverse temperature, and the static dielectric constant of ammonia is $\epsilon_s = 22$ at this temperature. This makes the MAS a strong electrolyte in this concentration range, and the static Coulomb interactions are already screened when the MIT occurs, and therefore cannot be its origin. The short-range interactions between electrons are also unlikely to be responsible for the MIT and the phase separation, because the mean distance between electrons is still about 12 Å at the relevant concentration 4 MPM, which is enough to neglect any overlapping between the wave-functions of the electrons localized in their ground state. The origin of the MIT must be found elsewhere, and a reasonable hypothesis is that it results from quantum momentum fluctuations of the solvated electrons. These ones are self-trapped quantum particles, whose dipolar momentum effectively fluctuates due to their quantum nature, with a characteristic frequency $\omega_0(T)$. This frequency corresponds to electronic transitions of the electrons between two states bound in their own trap potentials. They are experimentally detected by ordinary optical absorption measurements. The latter reveal a broad absorption line peaked at $\omega_0(T) \sim 0.9$ eV at low concentration and $T = -70\,^{\circ}\mathrm{C}$. For a given temperature, the maximum of optical absorption shows a pronounced red shift at metal concentration above 0.1 MPM, which cannot be caused by short-range or static Coulomb interactions as it has been discussed above. The frequency $\omega_0(T)$ characterizing the solvated electron state, is a significant phenomenological parameter of our theory. It is associated to the static polarizability $\alpha_0(0) = e^2/m\omega_0^2 \sim 913\, a_0^3$ of a solvated electron. Here, m and e are the electron mass and charge, while $a_0 = \hbar^2/me^2$ is the Bohr radius. We see that $\alpha_0(0)$ is a huge polarizability with respect to the one of a single ammonia molecule $\alpha_{\mathrm{NH_3}} \sim 18.8\, a_0^3$ [20] or that of a sodium ion $\alpha_{\mathrm{Na^+}} \sim 1.34\, a_0^3$ [21]. Therefore, these quantum fluctuations of isolated solvated electrons and their induced dipole–dipole interactions, which are nothing but their Van der Waals interactions [22], may have a dominant role in the MIT.

2. The state with solvated electrons

The key idea of Herzfeld was to evaluate the effect of the local field, with the help of the Clausius–Mossotti (CM) relation. Nevertheless, his calculation did not take into account the interactions between particles, which induce collective modes of polarization. Taking into account both the local field and the interactions effects, the CM relation may be generalized as [23,24]

$$\frac{\epsilon(T,\omega)/\epsilon_{\mathrm{NH_3}}(T,\omega) - 1}{\epsilon(T,\omega)/\epsilon_{\mathrm{NH_3}}(T,\omega) + 2} = \frac{4\pi}{3}\delta\chi(\omega) \tag{1}$$

where $\epsilon_{\mathrm{NH_3}}(T,\omega)$ is the temperature- and frequency-dependent dielectric function of pure ammonia, $\epsilon(T,\omega)$ is the similar quantity of the solution. $\delta\chi(\omega)$ is the change of susceptibility due to the dissolution of metal in the solvent. The susceptibility may be expressed in terms of an effective dynamical polarizability $\alpha(\omega)$ of a single solvated electron, by the relation $\delta\chi(\omega) = n\alpha(\omega)/\epsilon_\infty$. Hence, the problem focuses on the calculations of $\alpha(\omega)$. To overcome this barrier we choose a simple semi-analytical model suitable to calculate $\alpha(\omega)$ with a reasonable accuracy. The complete details of the model will be provided elsewhere, we just give here the main idea. It consists to separate classical degrees of freedom which are the ionic positions $\{R_i^+\}$ and the center of mass of the solvated electrons $\{R_j^-\}$, from the quantum fluctuating degrees of freedom of the electrons $\{u_j\}$ with respect to the $\{R_j^-\}$ (such that $r_j = R_j^- + u_j$ is the Cartesian coordinate of the electron j). After quadratic expansion of the Coulomb interactions with respect to the $\{u_j\}$, it appears three kinds of terms. First, the Coulomb interactions between the classical degrees of freedom, which might be treated by the classical theory of electrolytes. As we have seen, they are essentially screened. The second kind of interactions are the induced dipole–charge interactions. It may be shown that they vanish owing to the spherical symmetry of the liquid state. Finally, it remains the quantum induced dipole–dipole interactions, which result in Van der Waals attractions between the solvated electrons, and that we are looking for in the present paper. We thus consider MAS as a fluid of quantum particles localized in cavities with diameter $\sigma = 2r_c$, which interact through induced dipole–dipole interactions. They can be treated as a set of quantum Drude oscillators with isolated polarizability $\alpha_0(\omega) = e^2/m(\omega_0^2 - \omega^2)$. In the simplest approximation the interactions between particles can be cut off at small distances by the cavity size, whereas short-range details are ignored. Similar models of quantum polarizable fluids have been extensively studied [25–28], and we use the results which were previously obtained.

The problem is to evaluate the effective polarizability $\alpha(\omega)$. Due to the dipolar interactions between the oscillators, the polarizability $\alpha(\omega)$ is modified with respect to the non-interacting case and is given by the self-consistent equation:

$$\epsilon_\infty/\alpha(\omega) = \epsilon_\infty/\alpha_0(\omega) - 2E\big(\alpha(\omega)/\epsilon_\infty\big) \tag{2}$$

where the last term accounts the correlations between induced dipoles. Eq. (3) has been derived in [25], we only modify it by taking into account the high-frequency screening by the solvent (the use of ϵ_∞ in Eq. (2)). Formally the quantity $3\alpha E(\alpha)/\beta$ equates with the dipolar part of the internal energy per particle of a classical liquid of nonpolarizable particles with permanent dipole momentum $(3\alpha/\beta)^{1/2}$ [25,28], where β is the inverse temperature. Once the function $E(\alpha)$ is known, all the physical properties of the system can be evaluated by solution of Eq. (3). The simplest method to obtain $E(\alpha)$ is the Padé approximation [25,26], which is an interpolation between the case of low and large polarizability $\alpha(\omega)$. Adapting this method to our case, we get

$$E\big(\alpha(\omega)/\epsilon_\infty\big) = \frac{I_0(n\sigma^3)n\alpha(\omega)}{\epsilon_\infty\sigma^3 + I_1(n\sigma^3)\alpha(\omega)} \tag{3}$$

where $I_0(x)$ and $I_1(x)$ are analytical functions which depend only on a dimensionless density $x = n\sigma^3$ [28]. Replacing Eq. (4) in Eq. (3) leads to a quadratic equation, which allows complete calculations of both the real and the imaginary part of $\alpha(\omega)$:

$$\big[\epsilon_\infty I_1\big(n\sigma^3\big) - 2I_0\big(n\sigma^3\big)n\alpha_0(\omega)\big]\alpha^2(\omega) = \big[\epsilon_\infty^2\sigma^3 - \epsilon_\infty I_1\big(n\sigma^3\big)\alpha_0(\omega)\big]\alpha(\omega) - \epsilon_\infty^3\alpha_0(\omega) \tag{4}$$

The roots of Eq. (4) are complex, i.e. $\alpha(\omega) = \alpha'(\omega) + i\alpha''(\omega)$. The imaginary part is non-zero only in a finite range of frequency $\omega_-(T,n) < \omega < \omega_+(T,n)$ that corresponds to the dispersion of the collective polarization modes, regarded as a distribution of eigenvalues. Their density of states (DOS) is given by $D(\omega) \propto \omega\alpha''(\omega)$ [27]. For numerical evaluations, we use as input phenomenological parameters in Eq. (4): (i) $\sigma = 2r_c = 3.2$ Å [14] which remains fixed for all our calculations; (ii) $\epsilon_\infty = 1.76$ [29]; and (iii) $\omega_0(T)$ extracted from experimental data. This last parameter induces an implicit temperature dependence of $\alpha(\omega)$. From [30], we take $\omega_0(T = -70\,^\circ\mathrm{C}) = 0.86$ eV and $\partial\omega_0(T)/\partial T = -2.2 \times 10^{-3}$ eV/K for higher temperature ($-70\,^\circ\mathrm{C} < T < +70\,^\circ\mathrm{C}$). It allows us to calculate $\alpha_0(\omega)$ as needed in Eq. (4). Moreover, the static dielectric constant is calculated by taking $\epsilon_s(T = -70\,^\circ\mathrm{C}) = 25$, and $\partial\epsilon_s/\partial T = -0.1\ \mathrm{K}^{-1}$ [29] for the solvent. Fig. 2(a) illustrates our calculation at $T = -35\,^\circ\mathrm{C}$. At low concentrations, the DOS is peaked at $\omega_0(T)$, whereas the spectrum broadens progressively as the density n increases, indicating the drastic effect of the interactions.

Since our model is quadratic, the squared eigenfrequencies of the collective modes have to be positive. The approach of the low edge $\omega_-^2(n,T)$ to zero is an indication of the instability of the system. We define a critical density n_{c1} as

$$\omega_-(T, n_{c1}) = 0 \tag{5}$$

In the vicinity of n_{c1} (just above) the static dielectric constant diverges, indicating the onset of metalization. Thus Eq. (5) may be viewed as the generalization of the Herzfeld criterion for the polarization catastrophe and onset of metalization at n_{c1}. We have reported in Fig. 1 the calculated critical densities obtained with the use of Eq. (5). It indicates that the MIT occurs between 2 and 5 MPM depending on the temperature, which is quite comparable to the experimental data. The evaluation of the original Herzfeld critical density, i.e. without taking into account the interactions, provides the MIT located at about 14 MPM at $T = -70\,^\circ\mathrm{C}$. That shows how important the effect of the interactions is to correctly evaluate the MIT. As discussed above, another consequence of the polarization catastrophe is that the low-frequency dielectric constant $\epsilon(T,\omega)$ diverges in the vicinity of n_{c1} as it is experimentally observed in MAS [31,32]. Comparing the calculated data with the experimental ones, we find a good agreement between them (Fig. 2(b)). We also have calculated the real and the imaginary parts of the dielectric constant and evaluate the optical absorption coefficient $A(\omega)$. Again the calculated concentration dependence of $A(\omega)$ at the locus $\omega_{\max}$ of its maximum, agrees well with the experimental data [33,34] at concentrations below n_{c1} (Fig. 2(c)).

3. The metallic state with delocalized electrons

Above the critical concentration n_{c1}, the localized electrons are not stable. Hence, the behaviour of the system above n_{c1} depends on thermodynamics of the metallic state. This one is known to be unstable at sufficiently low

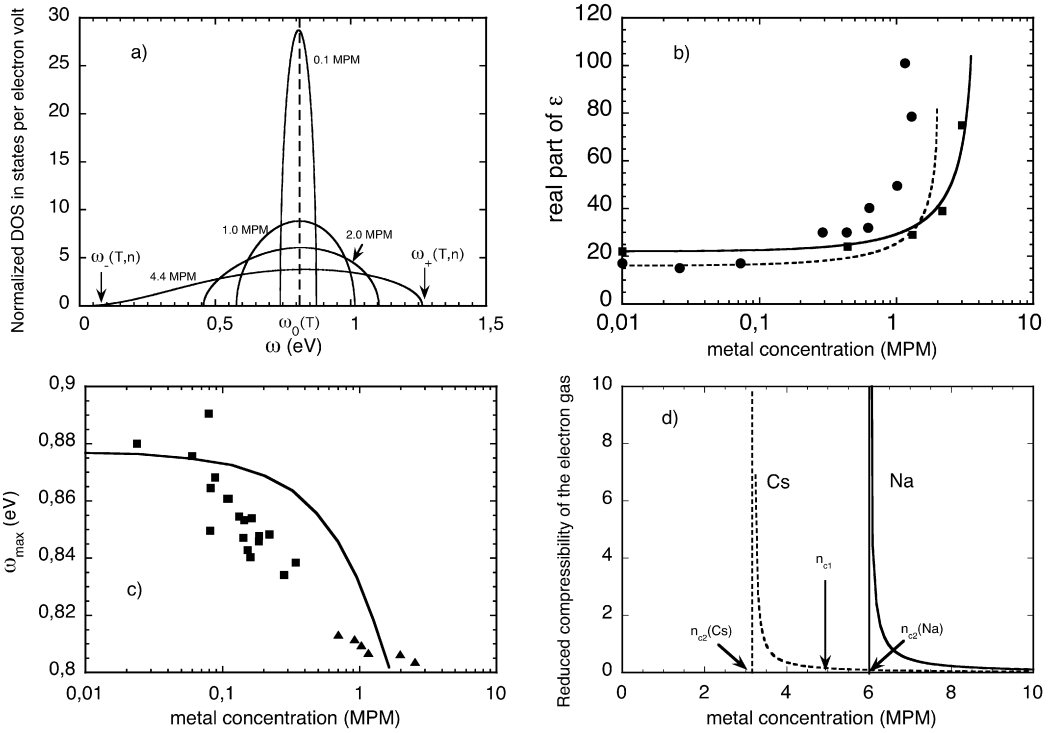

Fig. 2. (a) Normalized density of states (DOS) of the collective polarization modes of interacting dipoles, drawn for various metal concentrations at $T = -35\,^{\circ}\mathrm{C}$. The DOS is normalized to $\int D(\omega)\,\mathrm{d}\omega = 3$ (three degrees of freedom per particle). In (b) and (c): concentration dependencies of the dielectric constant (b) and the locus of the maximum of optical absorption (c). In (b) the square symbols correspond to the experimental data [31] on dielectric constant at $T = +20\,^{\circ}\mathrm{C}$, the circle symbols to that at $T = -35\,^{\circ}\mathrm{C}$ [32]. The solid and dashed curves show our results at $T = +20\,^{\circ}\mathrm{C}$ and $-35\,^{\circ}\mathrm{C}$, respectively. In (c) the triangle symbols indicate the experimental data on the absorption maximum in Na–NH_3 at $T = -65\,^{\circ}\mathrm{C}$ obtained from [33] and square symbols from [34], while the solid curve shows our results at the same temperature. In (d): reduced isothermal compressibility of the electron gas as a function of concentration at $T = -70\,^{\circ}\mathrm{C}$. The solid and the dashed curves correspond to the case of Na and Cs counterions, respectively. The arrow shows the locus of the dielectric catastrophe for the solvated electrons, indicating a miscibility gap between n_{c1} and $n_{c2}(\mathrm{Na})$ for Na, which does not occur in the case of Cs ions.

densities due to occurrence of a negative compressibility. Therefore, if the polarization catastrophe occurs at a lower density than this instability, it should provoke a phase separation. The MAS seems to be just this case. To reveal it, we have calculated the electronic part of the compressibility for the metallic state with the use of a modified model of stabilized jellium [35] for several alkali metals.

In a metallic state, the solution represents a plasma consisting of a degenerate electron gas strongly coupled with the ions dissolved in ammonia. Although a microscopic study of the system is still beyond possibilities of current methods, low temperatures and low metal concentrations of MAS simplify our analysis. We treat the influence of the solvent simply as a screening effect of the interactions, but we use different dielectric constants for the interacting electron gas and the ionic potential, because the latter are additionally screened by the orientational polarization of solvent molecules. We characterize the plasma by dimensionless parameters $r_s = (4\pi n/3)^{-1/3} a_0^{-1}$, $\Gamma_e = \beta e^2/\epsilon_\infty a_0 r_s$, and $\Gamma_i = \beta e^2/\epsilon_s a_0 r_s$, where $a_0 = \hbar^2/me^2$. We can express the change of the free energy caused by the dissolution of metal atoms in terms of the dimensionless parameters, and write the change Δf per electron (or per metal atom) as the sum of the electron, the ion, and the electron–ion contributions

$$\Delta f(n) = \Delta f_e(\Gamma_e) + \Delta f_i(\Gamma_i) + \Delta f_{ie}(\Gamma_e, \Gamma_i, r_s, a_i) \tag{6}$$

where a_i is a parameter related with the short-range electron–ion pseudopotential, which takes into account deviations from Coulomb interactions between electrons and ions. Because $\Gamma_e \gg \Gamma_i$, it may be checked that the electron gas

gives the main contribution to $\Delta f(n)$, whereas the ionic contribution is only a correction. We can thus ignore thermal effects for simplified evaluations. We take the expression obtained for the stabilized jellium model as in [35]:

$$\Delta f(n) = \frac{3k_F^2}{10} - \frac{3k_F}{4\pi\epsilon_\infty} + e_c(n) + \frac{C_M}{\epsilon_s r_s} + a_i n \tag{7}$$

where $k_F = (3\pi^2 n)^{1/3} a_0$ is the Fermi wave vector, and $C_m \approx -0.89774$ is the Madelung constant in atomic units (a.u.). The first, the second, and the third terms in Eq. (7) are the kinetic, the exchange, and the correlation contributions to the total energy of the homogeneous electron gas with a positive jellium background. The last two terms are corrections which take into account the atomic nature of the cations. The only difference with the stabilized jellium model [35], resides in the use of the dielectric constant in the relevant contributions. The local density approximation [36] was applied to calculate $e_c(n)$. The main difficulty is to evaluate a_i. The first attempt to provide it for MAS and account polarizability of ammonia molecules has been considered in [37]. In simple metals, the parameter a_i may be estimated as $\tilde{a}_i \approx 2\pi R^2/3$, where R is the ion-core radius related with the atomic number of the ion. Advanced models treating smooth continuous pseudopotentials [35] yield numerical corrections to this trend. We apply $\tilde{a}_i$ derived from [35] and take the polarizability of solvent into account, i.e. $a_i = \tilde{a}_i/\epsilon_\infty$. Importantly, we here use ϵ_∞ because a_i represents the short-range part of the interaction between electrons and ions. As a result, we find $a_i = 10.8$ and 26.1 a.u. for Na and Cs respectively. Numerical deviations of about 10 percent from these values do not change our results significantly. With the use of Eq. (7) we calculated the electronic part of the reduced isothermal compressibility $\kappa_F \sim [n\partial^2(n\beta\Delta f)/\partial n^2]^{-1}$ and found the concentration n_{c2} below which the electron gas is unstable. Fig. 2(d) shows the two curves obtained for Na and Cs respectively. In the case of Na, the compressibility κ_F diverges at a critical density $n_{c2} \approx 6$ MPM, whereas the dielectric catastrophe of the solvated electron state occurs at $n_{c1} \approx 5$ MPM. This is the origin of the miscibility gap and the associated phase separation: it exists a range of density $n \in [n_{c1}, n_{c2}]$ for which both states are unstable. Another consequence of this phenomenon is that a Mott mechanism for the MIT, which requires a stable electron gas at the critical density, appears impossible since the experimental MIT occurs at lower concentration than n_{c2}. The second curve in Fig. 2(d) is for Cs. It is seen in that $n_{c2} < n_{c1}$, contrary to the case of Na. No miscibility gap is thus expected in the case of Cs. This result is also coherent with the experimental facts. Although our estimations give upper and lower bounds for n_{c1} and n_{c2} respectively, underestimating the instability range, they reveal a correct trend in the dependence on the size of ions, namely, a decrease of the instability range for heavier ions, due to scattering of delocalized electrons on ion cores. The latter may decrease n_{c2} enough to destroy the miscibility gap.

4. Conclusion

Following the Goldhammer–Herzfeld idea and using the hard-sphere models for quantum polarizable fluids, we have evaluated peculiarities of MIT in MAS, namely, the anomalies of dielectric response and concentration changes in the absorption maximum. Our estimations of the behaviour of the insulating and the metallic phases have revealed an instability range at low temperatures. Our calculations tell us that MAS may deviate from the usual Mott scenario. At this stage, the theory is not complete. In particular, only the thermodynamics, which necessitates the evaluation and the comparison of different free energies, will allow us to determine all the lines of the phase diagram (spinodal lines for example), as well as the critical temperature. We reserve this problem for a next publication. We should also mention, that we have neglected one phenomenon: a possible pairing between the spins of two adjacent solvated electrons which seems to have been experimentally detected above $n \sim 1$ MPM [13]. We do not believe that this phenomenon influence so much the main features of the MAS phase diagram.

Finally, we also think that the proposed scenario may be applied to some other systems. For instance, in alkali metal–alkali halide solutions, solvated electrons, phase separation and dielectric anomalies were experimentally observed [38]. Another example is the case of doped polar solids such as oxides where formation of large polarons occurs. For such materials $\alpha_0\sigma^{-3} \sim \epsilon_\infty^{-1} - \epsilon_s^{-1}$ and the origin of the unusual behaviour is essentially due to different scales of screening at various frequencies $\epsilon_s \gg \epsilon_\infty$ like in the Wigner crystal of polarons [8]. The case of excitonic phase diagrams in usual semiconductors [39,40], could also be good candidates.

Acknowledgements

G.N.Ch. thanks the Leverhulme Trust for partial support of this work. P.Q. thanks B.K. Chakraverty and D. Mayou for many discussions concerning MAS.

References

[1] K.F. Herzfeld, Phys. Rev. 29 (1927) 701–705.
[2] D.A. Goldhammer, Dispersion und Absorption des Lichtes in ruhenden isotropen Koerpern; Theorie und ihre Folerungen (mi 28 Textfiguren), Teubner, Leipzig, Berlin, 1913.
[3] M. Ross, J. Chem. Phys. 56 (1972) 4651–4653.
[4] K.-F. Berggren, J. Chem. Phys. 60 (1974) 3399–3402.
[5] N.C. Pyper, P.P. Edwards, J. Am. Chem. Soc. 122 (2000) 5092–5099.
[6] B. Edwards, N.W. Ashcroft, Nature 388 (1997) 652–655.
[7] N.F. Mott, Proc. Phys. Soc. A 62 (1949) 416–422.
[8] S. Fratini, P. Quémerais, Eur. Phys. J. B 29 (2002) 41–49.
[9] G. Rastelli, S. Ciuchi, Phys. Rev. B 71 (2006) 184303.
[10] C.A. Kraus, J. Am. Chem. Soc. 29 (1907) 1557–1571.
[11] P. Chieux, M.J. Sienko, J. Chem. Phys. 53 (1970) 566–570.
[12] J.C. Thompson, Electrons in Liquid Ammonia, Oxford Univ. Press, London, 1976.
[13] P.P. Edwards, J. Supercond. 13 (2000) 933–946.
[14] J. Jortner, J. Chem. Phys. 30 (1959) 839–846.
[15] G.J. Martyna, Z. Deng, M.L. Klein, J. Chem. Phys. 98 (1993) 555–563.
[16] G.N. Chuev, M.V. Fedorov, N. Russo, Phys. Rev. B 67 (2003) 125103.
[17] G.N. Chuev, M.V. Fedorov, H.J. Luo, D. Kolb, E.G. Timoshenko, J. Theor. Comput. Chem. 4 (2005) 751–767.
[18] G.A. Thomas, J. Phys. Chem. 88 (1984) 3749–3751.
[19] J.C. Thompson, Rev. Mod. Phys. 40 (1968) 704–710.
[20] A.N.M. Barnes, D.J. Turner, L.E. Sutton, Trans. Faraday Soc. 67 (1971) 2902–2906.
[21] K.K. Mon, N.W. Ashcroft, G.V. Chester, Phys. Rev. B 19 (1979) 5103–5122.
[22] S. Lundqvist, A. Sjölander, Arkiv for Fysik 26 (1964) 17.
[23] G.M. Castellan, F. Seitz, Semiconducting Materials, Butterworths, London, 1951.
[24] T.G. Castner, N.K. Lee, G.S. Cieloszyk, G.L. Salinger, Phys. Rev. Lett. 34 (1975) 1627–1630.
[25] D. Chandler, K.S. Schweizer, P.G. Wolynes, Phys. Rev. Lett. 49 (1982) 1100–1103.
[26] K.S. Schweizer, J. Chem. Phys. 85 (1986) 4638–4649.
[27] Z. Chen, R.M. Stratt, J. Chem. Phys. 95 (1991) 2669–2682.
[28] L.R. Pratt, Mol. Phys. 40 (1980) 347–360.
[29] G. Billaud, A. Demortier, J. Phys. Chem. 79 (1975) 3053–3055.
[30] Farhataziz, L.M. Perkey, J. Phys. Chem. 79 (1975) 1651–1654.
[31] D.W. Mahaffey, D.A. Jerde, Rev. Mod. Phys. 40 (1968) 710–713.
[32] M. Schlauf, G. Schonherr, R. Winter, J. de Phys. IV 1 (1991) 185–190.
[33] W.H. Koehler, J.J. Lagowski, J. Phys. Chem. 73 (1969) 2329–2335.
[34] G. Rubinstein, T.R. Tuttle Jr., S. Golden, J. Phys. Chem. 77 (1973) 2872–2877.
[35] C. Fiolhais, J.P. Perdew, S.Q. Armster, J.M. MacLaren, M. Brajczewska, Phys. Rev. B 51 (1995) 14001–14011.
[36] J.P. Perdew, A. Zunger, Phys. Rev. B 23 (1981) 5048–5079.
[37] N.W. Ashcroft, J. de Phys. IV 1 (1991) 169–184.
[38] W.K. Freyland, K. Garbade, E. Pfeiffer, Phys. Rev. Lett. 51 (1983) 1304–1306.
[39] L.J. Schowalter, F.M. Steranka, M.B. Salomon, J.P. Wolfe, Phys. Rev. B 29 (1984) 2970–2985.
[40] L.M. Smith, J.P. Wolfe, Phys. Rev. Lett. 57 (1986) 2314–2318.